Wave–wave interactions, microseisms, and infrasonic ambient noise in the ocean

A. C. Kibblewhite and K. C. Ewans
Department of Physics, University of Auckland, Private Bag, Auckland, New Zealand

(Received 10 January 1985; accepted for publication 7 May 1985)

Underwater ambient noise is known to be wind dependent. Several mechanisms have been proposed to explain the nature of the transfer of energy from the wind to the acoustic noise field. Examples include wind and wave turbulence and nonlinear interactions between surface waves. This study examines these wind-related mechanisms at the low end of the acoustic spectrum. Data from a long-term investigation of ocean waves and the associated microseism response recorded ashore have provided evidence helpful in identifying the active processes. It is concluded that the noise field below 5 Hz is controlled by nonlinear wave–wave interactions and that existing theories account adequately for the effects observed.

PACS numbers: 43.30.Bp, 43.30.Lz, 43.30.Nb

INTRODUCTION

Studies of ambient sea noise have shown that levels in certain regions of the noise spectrum are related to local wind conditions. In his paper, Wenz[1] presented a generalized wind-dependent noise spectrum, which was supported by data from many experiments at frequencies above 200 Hz. Below 200 Hz, it was apparent that, in general, the sea noise level is controlled by nonwind related sources, such as biological, shipping, and other manmade industrial activity. However, later measurements at frequencies below 10 Hz have indicated that the wind can also have a considerable effect on noise levels in this part of the spectrum.[2]

Several mechanisms have been proposed to account for the transfer of energy from the wind to the ambient noise field at low frequencies. One of these considers that the noise source lies in turbulent pressure fluctuations in the atmospheric boundary layer.[3–7] A second considers the role of nonlinear interactions between ocean surface waves,[3,8–15] and a third examines the interaction of both surface waves and turbulence.[16]

Because reported ambient noise data are sparse at frequencies below 10 Hz, it has been difficult to assess the agreement between theory and experiment. However, a significant contribution was made recently when Nichols[17] presented new data and made comparisons with both theory and other relevant experimental results. While the lack of detailed environmental data did not permit definite identification, his summarized evidence suggests that nonlinear wave–wave interactions and/or turbulence are the most likely noise generating mechanisms.

For reasons outlined later, long-term wave recordings have been carried out on the west coast of New Zealand to establish the general nature and characteristics of the wave field in the area. The particular region, however, possesses certain unique features helpful to the examination of more specific ocean-wave phenomena, and the general program was expanded.

The particular supplementary study on which this paper is based has been concerned with the role of wave–wave interactions in the generation of both wave-induced microseisms and the ocean ambient noise field at very low frequencies. In spite of the vast literature on the subject,[11,18–23] debate persists as to the precise nature of the mechanism of microseism generation,[18–20] and, as discussed earlier, similar ambiguity exists concerning the source of the noise field in the infrasonic region. Because nonlinear wave–wave interactions are also invoked to account for the self-stabilization of the ocean-wave spectrum,[24] a parallel investigation has been concerned with the growth and decay of the ocean-wave field. A third study has involved an assessment of the extent to which local sea state can be monitored using land based sensors, as has been done elsewhere in a less complicated environment.[25]

These studies are obviously closely related and it was considered that all might be profitably addressed in this particular geographical region through a correlation of sea state and the seismic response it generates. Existing seismic data in the 0.1- to 2-Hz range show that a close relationship exists between the sound pressure at the seafloor and the seismic ground response.[21–23] Further, while the seismic amplitude spectrum will depend on both the source spectrum and the transfer function of the ocean/seabed system,[3] the restricted geophysical data available for the region of this study[26] and the results of some preliminary measurements suggested that the transfer function would not unduly distort intercomparisons over the frequency range of interest. (In another study to be reported, the ocean-wave and seismic measurements were supplemented by recordings of the ambient noise field, but, in the present study, no hydrophone was available.)

Much of the detail of the analysis carried out will be more appropriately reported in companion papers. However, some of the results obtained provide a timely supplement to Nichols' review[17] and appear to justify presentation in this forum.

I. BACKGROUND TO THE MEASUREMENT PROGRAM

A. The Maui Development Environmental Program

In 1969, a major natural gas and condensate field was discovered off the west coast of the North Island of New Zealand (Fig. 1). Because the Maui field, as it has been

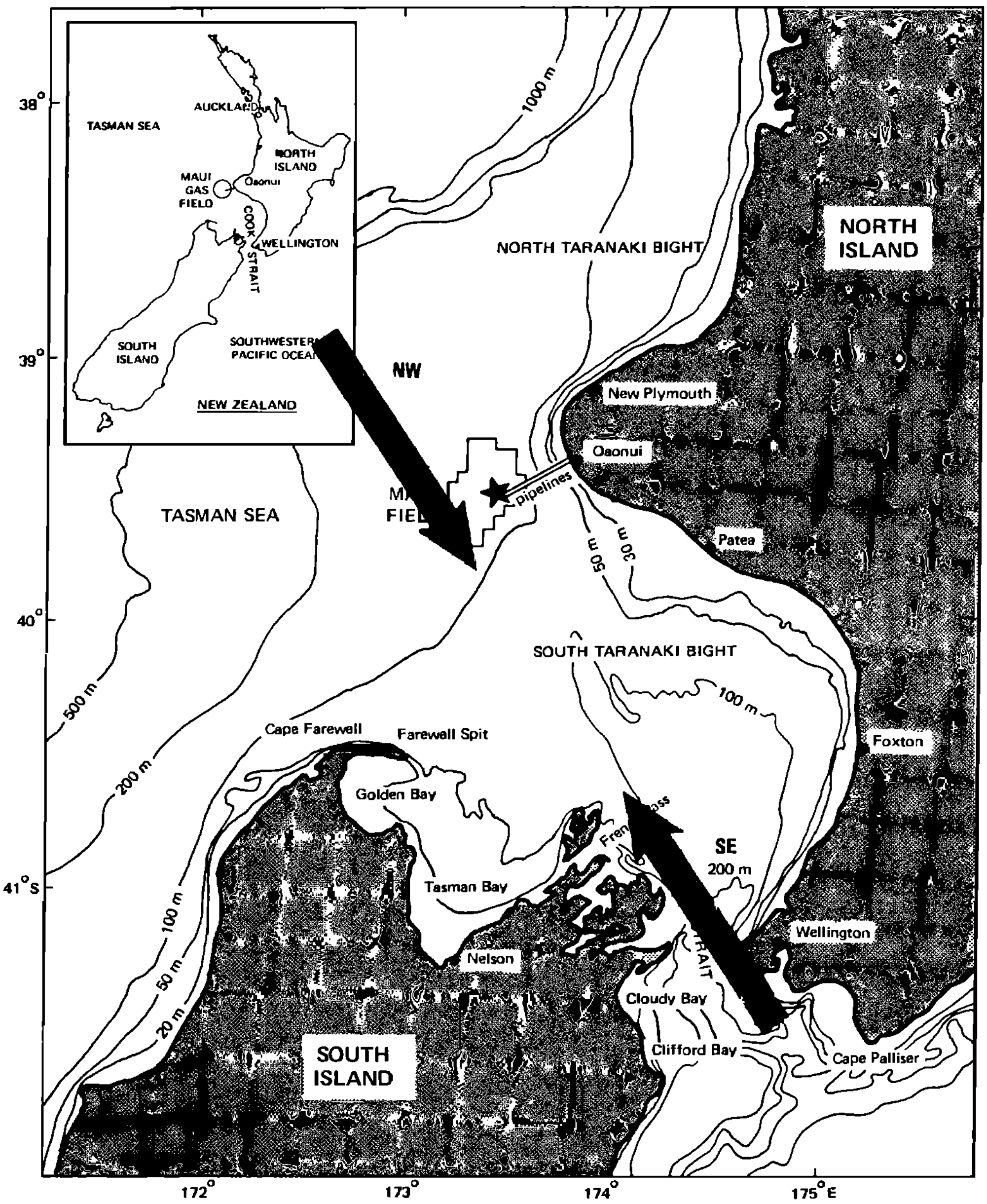

FIG. 1. Localities and bathymetry of Cook Strait and the Maui environment. The Waverider buoy is installed close to the Maui platform and the receiving instrumentation ashore at Oaonui.

named, is some 30 km from the coast in water depths around 100 m, the commissioning of it has involved a major offshore engineering operation. Through concern for the environment, the company responsible for the undertaking commissioned a study of the characteristics of the Maui seas to establish any impact of the engineering operation on the region.

The Maui Development Environmental Study[27] involved programs in physical and chemical oceanography, coastal geology, and marine biology. A major element of the physical oceanography program has been the wave-climate investigation referred to earlier. Preliminary reports on some of the wave properties established in the early part of the program have been presented already,[28,29] but more extensive analyses, based on the larger data file which now exists, are being prepared as a new series, of which this paper is one.

The preliminary analysis established that the wave field can vary significantly throughout the Maui region due to the orographic influence of Cook Strait. New Zealand is subject to a regular succession of weather systems which cross the country from west to east. The mountain chain running roughly NE/SW and centered on Cook Strait acts as a barrier to the air flow associated with these systems and produces funneling effects and strong winds in the Cook Strait and Maui region. Further, as the weather systems pass across the country, the Cook Strait area experiences well-defined changes in the wind field, the wind vector often swinging quickly through approximately 180° from the northwest to the southeast.

These regularly occurring southeasterly events were early recognized as providing ideal conditions for the study of ocean-wave phenomena. Not only are the wind changes well defined and repetitive, but the west coast of the North

Island, just north of Cook Strait, presents an almost orthogonal coastline to the southeast winds, and the overall area defines a constant fetch of approximately 200 km at the Maui platform.

B. Instrumentation and procedures

Details of the instrumentation employed are available elsewhere,[27,30] and only a brief description is given here.

The wave data were provided by a Datawell Waverider buoy (known as Maui-A) moored in approximately 110 m of water, close to the Maui platform. The signal from this unit was received ashore 30 km away and the analog output representing sea-surface displacement was recorded on an instrumentation tape recorder. Also recorded was the output of a Teledyne Geotech SL210 long period seismometer installed at the receiving site, and a time code signal. Recordings of a 20-min duration were initiated automatically every 4 h. In addition to the magnetically recorded data, the raw analog wave signal was processed to provide a continuous record of significant wave height and mean zero-crossing period. Meteorological parameters for the Maui regions were provided by the NZ Meteorological Service.

Spectral analysis of the magnetic tape recordings of sea-surface and ground displacement was effected on a Unigon dual channel FFT processor (model 4520) and a PDP-11 computer in two stages.

In stage 1, the tapes were replayed into the FFT processor and the processed data transferred to the PDP-11 and storage. The wave and seismic signals were processed together. The frequency analysis range and playback tape speed were such that the effective frequency analysis range was 0–1 Hz with a spectral resolution of 1.17×10^{-2} Hz.

The 20-min recordings allowed an average of three consecutive maximally overlapped sweeps to be obtained. The procedure followed was to transfer each of the three average spectra to the PDP-11, scrutinize for quality, and then compute the final spectrum as the average of these three. The spectra were then stored on file in daily lots of six spectra for stage 2 of the analysis procedure.

Stage 2 involved spectrum scaling, parameter computation, and plotting. The raw spectra stored from stage 1 were scaled to have units of variance density (m^2/Hz) and a number of basic output parameters were also computed.

The wave and seismic spectra were plotted over the frequency bands 0.03–0.5 and 0.095–1.0 Hz, respectively, and presented initially according to their GMT recording time. Various presentations were developed from this format as required.

C. Nonlinear surface-wave interactions

The solution of the linearized equations of hydrodynamics produces the well-known expressions for gravitational and capillary surface waves and the subsurface effects they produce. The internal disturbances, such as pressure and water-particle movement, decay rapidly with depth and are negligible at a depth of the order of a wavelength. If second-order terms are considered in the hydrodynamic equations, other effects appear. In particular, as first reported by Miche,[8] the generation of very low-frequency pressure fluctuations due to the nonlinear interaction of opposing waves on the ocean surface can occur. The distinctive features of these waves are that the pressure effects they produce do not decrease with depth, occur at twice the surface wave frequency, and are proportional to the amplitude product of the interacting waves producing them.

Miche's theory was developed by Longuet-Higgins[9] in providing an explanation for the ocean-induced component of the microseism field. This analysis, still related to microseisms, was expanded further by Hasselmann,[3] Nanda,[10] and Darbyshire and Okeke[11] in particular. With the recent interest in the ocean ambient noise field at frequencies below 10 Hz, Miche's basic theory has also been considered by Brekhovskikh,[12] Harper and Simpkins,[13] Hughes,[14] and Lloyd[15] in seeking a theoretical basis for the observed acoustical spectrum at low frequencies and its relation to surface-wind conditions.

Apart from small inconsistencies, which have been clarified by Lloyd, the theoretical predictions for the pressure field produced by nonlinear interactions are essentially the same in all treatments—Hasselmann (Ref. 3, Eq. 2.15), Brekhovskikh (Ref. 13, Eq. 53), Hughes (Ref. 14, Eq. 33), and Lloyd (Ref. 15, Eq. 35).

When the contribution from capillary waves is ignored, the expression for the one-dimensional power spectrum of the pressure field $Sp(\omega)$ can be written in the form

$$Sp(\omega)=\frac{\pi\rho^2g^2\omega^3}{2c^2}\,[Sa(\sigma)]^2\int_0^{2\pi}G(\theta)G(\theta+\pi)d\theta, \quad (1)$$

where ρ is the surface density of seawater, c the ocean sound velocity, σ the angular frequency of the surface wave, $Sa(\sigma)$ the power spectrum level of the surface wave displacement, and the function of θ describes the directional properties of the wave field. Following Lloyd,[15] and using the value for the integral adopted by Hughes,[14] Eq. (1) reduces to

$$Sp(f_a)=(2\pi^3\rho^2g^2/c^2)f_W^3\,[Sa(f_W)]^2, \quad (2)$$

where f_a and f_W are the frequency of the components of the acoustic pressure and gravity wave fields, respectively, and the integral equals $\frac{1}{8}$.

To obtain the displacement spectrum, $Su(\omega)$, relevant to the seismic measurements, the exciting pressure field must be modified by the transfer function of the layered medium so that in terms of Eq. (1),

$$Su(\omega)=\pi(\rho^2g^2/c^2)K_1\,T_u^n(\omega)\omega^3 \times[Sa(\sigma)]^2\int_0^{2\pi}G(\theta)G(\theta+\pi)d\theta, \quad (3)$$

where K_1 is a factor involving the active area of the nonlinear interactions and the distance from the sensor, $T_u^n(\omega)$ is the transfer function for the vertical displacement of the elastic half-space, and n is the mode number.

Hasselmann[3] examines the properties of $T_u^n(\omega)$ for a particular environmental model and gives a curve for the ratio of the effective transfer function to the transfer function for the Rayleigh mode alone, $T_u^n(\omega)/T_u^R(\omega)$—his Fig. 3. $T_u^R(\omega)$ is proportional to frequency and the constant of proportionality is governed by the elastic properties of the half-space. Thus the frequency dependence of T_u^R has to be taken into account when considering absolute values. The overall frequency dependence will depend on the shape of the curve relating T_u^n/T_u^R to the nondimensional frequency, $\omega H/2\pi c$ (H = water depth)—see Hasselmann, Figs. 2 and 3. In the simplest case, the maximum of this ratio curve will be well above the frequency range of interest here and the simple ω dependence of the Rayleigh transfer function will apply. In this case, we can write

$$Su(\omega) = \pi \frac{\rho^2 g^2}{c^2} K_1 K_2 \omega^4 \, [Sa(\sigma)]^2 \int_0^{2\pi} G(\theta) G(\theta + \pi) d\theta, \quad (4)$$

where K_2 is a constant associated with the Rayleigh transfer function.

For this simplest case, therefore, it follows that: (1) there should be a two-to-one frequency relationship between the seismic and ocean-wave spectra; (2) the power spectral levels of the vertical component of the ground displacement should be proportional to the square of the power spectral levels of the ocean-wave field; and (3) the ratio $R_s = Su(\omega)/[Sa(\sigma)]^2$ should display a fourth-power dependence on frequency.

II. GENERAL RESULTS

A. Basic correlations

Sea-wave/microseism correlations in the Maui region give clear evidence for the marine generation of microseisms in the frequency range 0.05–1.0 Hz. Comparison of any sea spectrum and its seismic equivalent will identify peaks in the wave spectrum with corresponding peaks in the microseism spectrum at or very close to twice the frequency. A primary frequency peak in the seismic spectra at the same frequency as the sea waves has also been identified in a special measurement program, but, because its level is two orders of magnitude below that of the double frequency secondary peak, it is not routinely observed in the magnetic tape recordings.

The meteorology of the western Tasman Sea controls the wave climate in the Cook Strait region and, hence, the microseismic response. If calm weather prevails for some time, the sea-wave spectrum is then characterized by a single peak at about 0.07 Hz, produced by a persistent swell arriving from the southwest out of the Southern Ocean. The microseism spectrum has a corresponding peak at double this frequency. If a local wind then arises, it is first evident as low-level, broadband energy at the high-frequency end of the wave spectrum. The microseism spectrum shows components at twice these frequencies. If the local sea continues to grow, the components in the sea spectrum will increase in amplitude and the associated peaks will shift to lower frequencies. If the wind persists long enough, the frequency of this peak approaches that of the long period swell and usually swamps it, the two components merging in a large peak at low frequencies. The frequency at which this occurs is often around 0.11–0.12 Hz in the wave spectrum and 0.22–0.25 Hz in the microseism spectrum. However, whereas the wave spectral levels will increase by several times during this process, the microseism levels can increase by several orders of magnitude.

A comprehensive review of all aspects of wave/microseism behavior observed in the course of this study is presented elsewhere.[30] In this paper, we restrict discussion to results relevant to the identification of those effects occurring at the ocean surface, which generate the pressure field responsible for the acoustic ambient noise levels and microseisms at very low frequencies. This will lead us in particular to a discussion of periods of activity associated with southeasterly events.

B. Selected SE events

In the Introduction, reference was made to those features of Cook Strait which generate SE meteorological events and which make this region particularly suitable for ocean-wave studies. It will be instructive to develop this analysis in terms of a few such events, selected from those observed over the 3-year period in which recordings have been made. While these specific events have been selected because they tell the story most clearly, the general wave/microseism behavior described is characteristic of all such events. Descriptions of others are available elsewhere.[30]

1. Event 16–20 October 1981

a. Brief description of the meteorology for the period. Over the period 13–14 October, a large anticyclone covered New Zealand. In the Maui region, the winds were dominantly westerlies at around 10–15 m/s (20–30 kn). As the anticyclone moved eastward on the 15th, the winds veered slowly north about to lie in the northerly quarter early on 16 October. During that day, a low-pressure system developing to the south moved rapidly on to the country. A front associated with this system crossed the Cook Strait region about midday. The wind shifted rapidly and stabilized around the bearing 135 °T(SE) early on 17 October (see Fig. 2). This shift in bearing was accompanied by an increase in speed to over 30 m/s. The depression continued to move eastward over the next two days. The wind remained from the southeast, but the wind speed decreased steadily to less than 5 m/s on 20 October, by which time another anticyclone covered the country.

Over the next few days, New Zealand was dominated by this anticyclone. The winds in the Maui region were more or less constant from the north and slowly increased to about 15 m/s by 22 October. At this time, another low-pressure system moved on to New Zealand, and the pattern of 16 October was essentially repeated. The winds again swung north about to steady once again in the southeast quarter. This change was again accompanied by an increase in wind speed (to over 30 m/s), followed by a drop to less than 5 m/s 24 h later.

b. Spectral histories of the wave and microseism fields. The behavior of the ocean-wave and microseism fields is best discussed in terms of the spectral contour plots for the period [Fig. 2(a) and (b)].

On 14 October, the ocean-wave field at the Maui platform is characterized by the low-frequency swell (0.07 Hz) from the southwest and the development of a local westerly sea under the influence of the increasing westerly winds. The

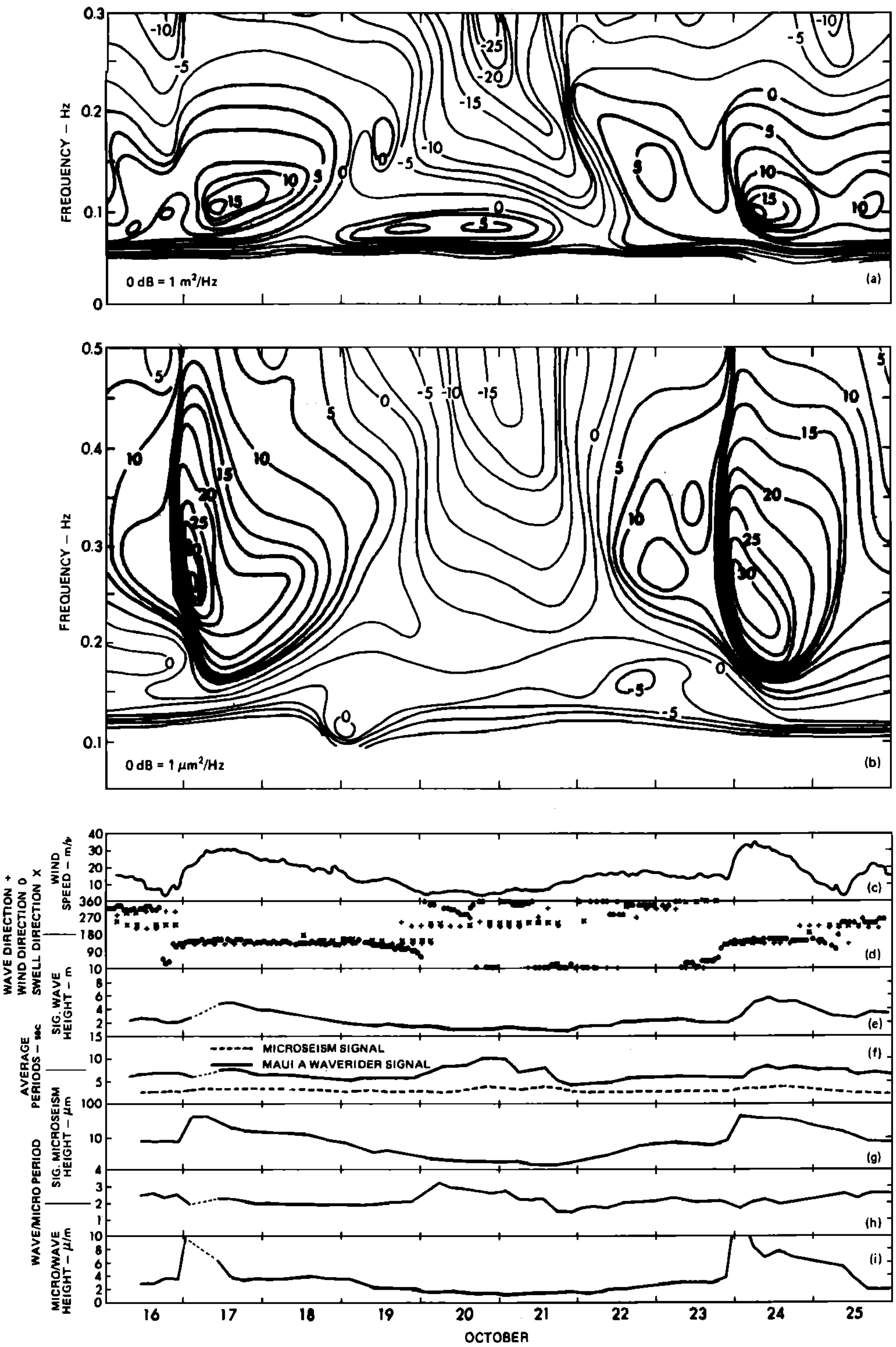

FIG. 2. Time series plot of wind, ocean-wave, and microseism parameters for the period 16–29 October 1981. From the top: (a) ocean-wave spectral history; (b) seismic spectral history; (c) wind speed, m/s; (d) wind direction O, wave direction +, swell direction, ×; (e) significant wave height in m; (f) average wave and microseism period; (g) significant microseism height, in μm; (h) wave/microseism period ratio; and (i) ratio of microseism to wave height, μ/m.

spectral levels of this local sea begin to decrease early on 16 October as the wind shifts slowly in bearing and decreases in intensity.

Early in the afternoon of 16 October, the spectral levels increase sharply in response to the episodic event of that day, in which the wind swings rapidly to the southeast and increases to nearly 30 m/s. A new low-frequency peak in the wave spectrum has been established by midday on 17 October, and this is sufficiently strong to mask the low-level southwesterly swell. Thereafter, this peak increases in frequency, and all spectral components decrease in level as the winds decrease slowly over the next three days.

Throughout 14–15 October, the microseism noise field first increases and then decays in response to the changing local westerly sea. The peak of the activity moves to lower frequencies throughout 14 October in step with the growth of the wave field, the activity extending to frequencies beyond 1 Hz. The actual 4-hourly spectra for this period are quite irregular in form, a characteristic invariably found with growing and decaying wave fields (see Fig. 3). Through-

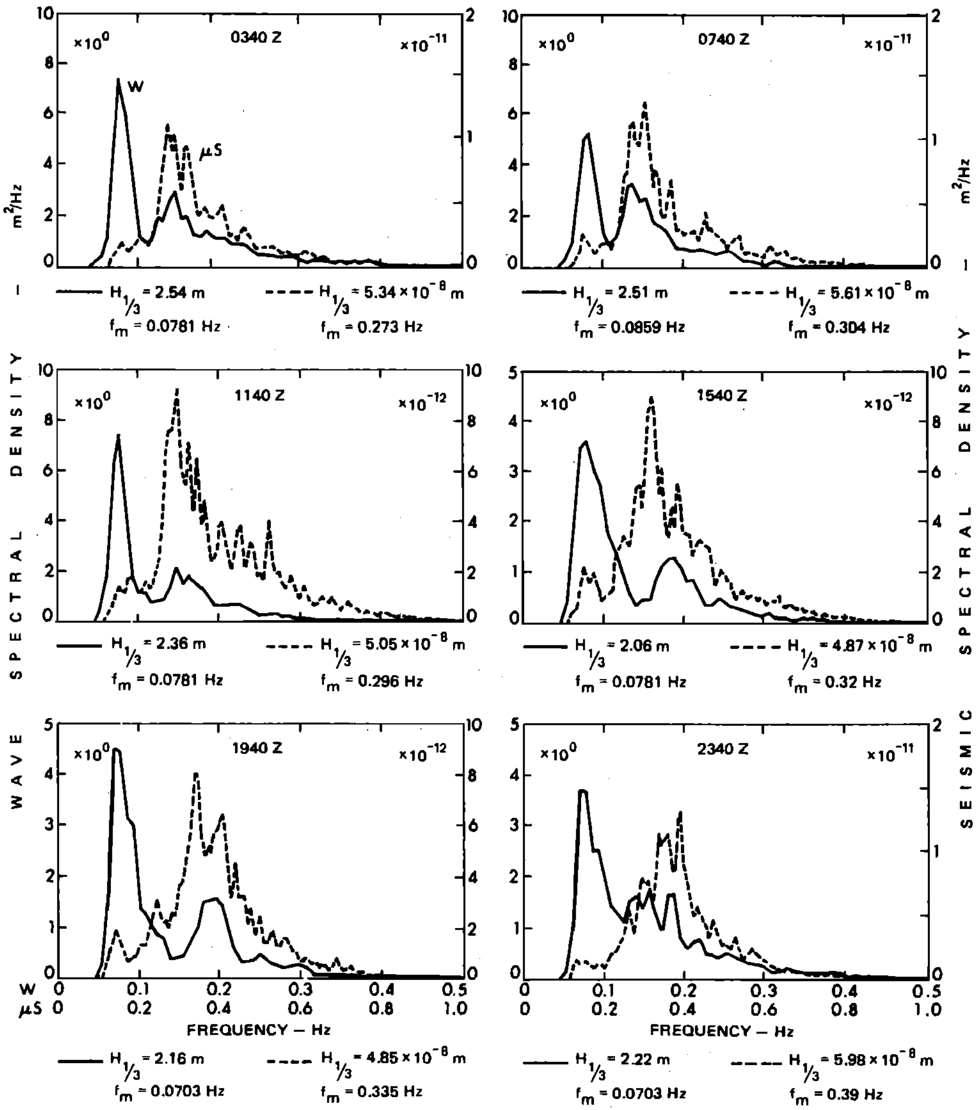

FIG. 3. Selected 4-hourly wave and microseism spectra for 15 October 1981.

out this period, the activity associated with the growing local sea dominates the microseism signal associated with the low-frequency swell. The latter is, nevertheless, clearly apparent in the wave spectra of 15 October, but barely discernible in the microseism spectra for that time.

The wind change on 16 October produces a major and characteristic response. The initial decrease in wind speed results in a decrease in wave spectral levels. However, because of the shift in wind bearing in this interval, the seismic spectral levels increase over a broad frequency band, and then jump dramatically (by 20 dB) with the rapid increase in wind speed at 2400 h (see Fig. 2). Associated with this increase, the spectral peak moves rapidly to lower frequencies, roughly in step with the peak in the wave field. As the two spectra grow to their maximum development, they become narrower and smoother. The narrower the spectra become, the closer to an exact 2:1 frequency relationship do the spectral peaks conform. A close 2:1 correspondence exists by 1940Z 17 October and persists throughout the next day. Gradually, however, both the ocean-wave field and seismic noise field decay in level, in response to the decreasing wind. This decay is accompanied by a shift in the spectral peaks to higher frequencies.

The significance of the shift in wind bearing during a southeasterly event is brought out clearly in the plot of the environmental parameters in Fig. 2. In particular, the ratio of the microseism/wave activity [2(i)] shows a pronounced peak at this time. Another example occurs with the event on 23 October in the same figure.

The joint behavior of the ocean-wave and seismic spectra can be interpreted in terms of wave–wave interactions. These occur in two forms, the first involving interaction between the spectral components of two opposing seas as originally conceived by Longuet-Higgins[9,31] and the second involving interactions between components of a single active sea. The second form is a consequence of natural spreading of the wave energy and has already been proposed by Tyler *et al.*[32] as a mechanism for the generation of microseisms. Here, only an abbreviated interpretation of the effects observed is given, but a detailed analysis is available elsewhere.[30]

Referring first to the event of 17 October, the rapid increase in wind speed (to approximately 30 m/s) and change in bearing from northwest to southeast (approximately 180°) bring a rapidly developing southeasterly sea into direct opposition with the original high-level wave energy from the northwest [significant wave height is approximately 3 m; see Fig. 2(e)]. Moreover, as the generating area for the latter covered a large part of the north Tasman Sea, it persists for some time in spite of the strength of the southeasterly winds. A classic situation therefore exists for the development of wave–wave interactions of the type envisaged by Brekhovskikh and others, and the generation of the associated pressure field. Microseism spectral power levels reach the order of 10^{-9} m^2/Hz, and the power ratio of the spectral peaks around 200–300 $(\mu/\mathrm{m})^2$, during the early part of this and other comparable events.

At 0800, the high seismic activity at frequencies above 0.25 Hz drops rapidly to lower and steadier levels, even though the wind reaches its highest speed about this time, and the southeasterly sea its maximum development. This decrease in seismic level, which occurs without a comparable change in the spectral levels of the local sea, is believed to reflect the demise of the initial northwest sea and a sharp decline in this form of wave–wave interaction. The lower level of activity which follows is believed to be associated instead with nonlinear interactions between opposing spectral components in the new southeasterly sea, the existence of which is a consequence of angular distribution of wave energy within the active sea. During this phase, the wave and seismic spectral levels in the region of the peak remain roughly constant. The levels during this type of interaction are typically around 10^{-11} m^2/Hz and the power ratio of the spectral peaks around $10(\mu/\mathrm{m})^2$. Both values are an order to magnitude lower than those associated with the more energetic processes invoked when two distinct wave fields are in opposition.

As the wind decreases, the spectral levels slowly fall and the peak frequency shifts to higher frequencies. On the other hand, during development of a new sea, under a changing wind regime, the wave spectrum usually lags on the seismic field. It is now clearer why the seismic spectrum (and general wind-induced ambient noise field) correlates more closely with the wind than the sea state. Close correlation with sea state is only to be expected under steady-state conditions.

The sequence of 21–25 October, also shown in Fig. 2, can be interpreted similarly.[30]

III. SUPPLEMENTARY EVIDENCE

A. Spectral overlap and wave–wave interactions of opposing seas

In most southeasterly events, the switch in wind direction, increase in wind speed, and growth of the southeasterly sea, take place so rapidly that the 4-hourly recordings on which the routine sampling is based, rarely allow the detail of the spectral development and decay to be resolved. The events of October 1981, analyzed above, are typical in this regard (see Fig. 4). In other events, however, the wind changes take place sufficiently slowly for the essential features of the development to be resolved. In such cases, an examination of the spectra shows that the seismic activity occurs essentially in the range-of-frequency overlap of the two spectra. The dominant seismic signal is generated by the interaction of the two wave trains.[30]

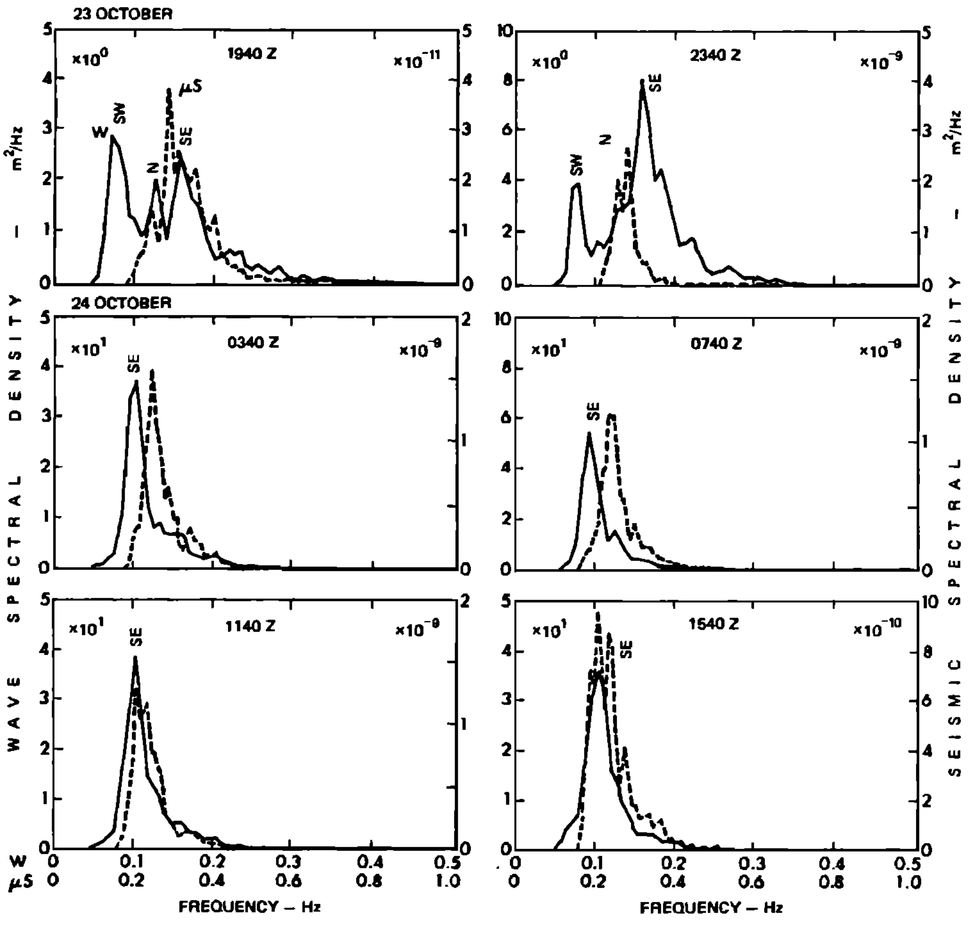

FIG. 4. Four-hourly spectra for the event of 23 October 1981.

B. Microseism level dependence on ocean-wave amplitude

According to theory [Eq. (4)], there should be a square-law relation between two corresponding spectral levels when appropriate account is taken of the frequency term in the expression. However, while an inspection of the experimental data clearly indicates some power law dependence between the seismic response and the ocean-wave field, complexities in the latter and distortions arising when the frequency relationship between the two fields was not exactly 2:1, obscure an examination based on spectral levels. It proves more informative to consider the relationship between the ocean waves and their seismic response using the connection between the two provided by Longuet-Higgins' original formalism.[9]

According to Longuet-Higgins, the double frequency microseism amplitude is proportional to the product of the amplitudes of the oppositely traveling ocean waves producing them, and also proportional to the square of their frequency. If the opposing waves are from the same field, such as in the case of those within an active sea with a cosine angular distribution, then the microseism amplitude is proportional to the square of the amplitude of the ocean waves generating them. A convenient and reliable measure of the amplitudes can be obtained from the significant heights derived from the zeroth moment of the two spectra. In addition, the ocean-wave mean period can be calculated from the ocean-wave spectrum. If compensation is made for this period dependence, the actual amplitude dependence can be checked.

When various analyses were applied to a two-year data set, the square-law dependence of the amplitudes was confirmed to within the statistical uncertainties involved.[30] As an example, a plot of the logarithm of the microseism significant height, compensated by the square of the mean ocean-wave period versus the logarithm of the ocean-wave significant height for all the spectral data for the years 1980 and 1981, is given in Fig. 5. The shape and spread of the data points follow a broad band with a slope comparable with the continuous line, which has a slope of 2. A least-square regression fit actually establishes the slope of the 1586 data points as 1.6 (correlation coefficient 0.82), but other and more selective analyses involving bandlimited spectra confirm the square-law relationship.[30]

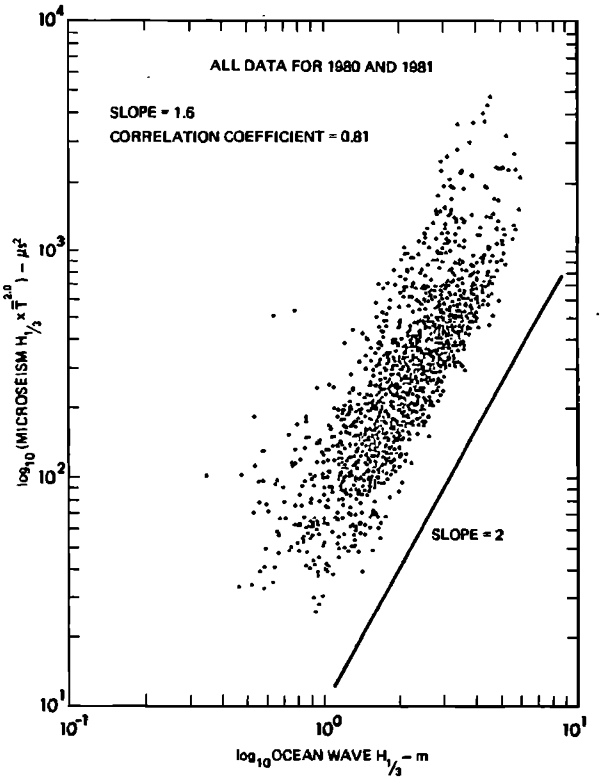

FIG. 5. Relationship between the seismic and wave significant heights for all spectra in the 1980–81 database.

C. Microseism level dependence on ocean-wave frequency

The dependence of the microseism level on the ocean-wave frequency can also be examined through the two formalisms. In Longuet-Higgins' analysis,[9] the microseism amplitude is shown to be dependent on the square of the ocean-wave frequency, while in the formalism of Eq. 4, the seismic spectrum level at any frequency is related to the fourth power of the wave frequency and the square of the ocean-wave spectrum level.

Attempts to establish the frequency dependence through Longuet-Higgins' formalism using significant heights were not successful because of the limited range of values in the mean zero-crossing period. Through Eq. (4), the dependence could be tested by plotting the logarithm of the ratio $R_s = Su(\omega)/[Sa(\sigma)]^2$ against the logarithm of the frequency. Alternatively, one can establish the dependence of the ratio on frequency by measuring the spectral slopes of the two related spectra in the equilibrium range above the spectral maximum. While both procedures are applicable, it proved more effective to examine this question through an approach based on nondimensionalized spectra. This approach had been applied successfully to the wave spectra in order to establish properties of the wave field, and it was extended to the microseismic spectra. For details, the reader is referred elsewhere,[30] but, essentially, a nondimensionalizing procedure based on that of Hidy and Plate[33] was used. As Liu[34] had found this scheme to give a universal function for steady(S), growing(G), and decaying(D) wave conditions, it was considered appropriate to apply the nondimensionalization in the present case to spectra grouped according to various classifications.

The nondimensionalization involves multiplying the variance spectral density function by the peak frequency f_m and dividing by the variance m_0. Each spectrum in a particular group was nondimensionalized in this way and the group was then averaged to arrive at the universal spectral function $\psi(f/f_m)$ for the group. This average spectrum was then curve fitted with the normalized JONSWAP function[30,35] to give a new function $\tilde{S}(\tilde{f})$. Various parameters were derived from this best-fit curve for other studies. For the present analysis, measurements of the spectral slope were made for various intervals at frequencies above f_m by performing a linear regression analysis on $\log_{10}\tilde{S}(\tilde{f})$ as a function of $\log_{10}\tilde{f}$.

These intervals were selected by a visual inspection of the normalized spectra. As an example, the nondimensional spectra for the S group (SE winds) are given in Fig. 6.

The first feature apparent in the processed spectra is that, for local seas, both the ocean-wave and seismic spectra are apparently well described by a universal function under the Hidy and Plate nondimensionalization. Moreover, the spectra for decaying, growing, and steady conditions are all found to be similar under this nondimensionalization. The evidence suggests further that the spectra were rather similar irrespective of the bearing of the exciting sea. This implies that microseism generation is effected by ocean waves at all frequencies and that no preferential generation or propagation frequency prevailed.

The second apparent feature is that the universal functions for the wave spectra suggest the existence of a double equilibrium range, with slope values roughly the same in all groups. For f/f_m in the 2–3 range, the spectrum level dependence on frequency is about f^{-4}, while, above $f/f_m = 3$, the proportionality is closer to f^{-5}. This result, which has its parallel in work by Forristal,[36] is discussed further by Ewans.[30] In the present context, this property of the spectra was recognized in evaluating the slope of the spectral curves above f_m. On the basis of Eq. (4), it might then be expected that two regions would exist in the high-frequency region of the microseism spectra, with frequency dependencies of f^{-4} and f^{-6}, respectively.

In general, most of the microseism spectra also displayed two regions with different slopes, although the point at which this occurred was closer to $f/f_m = 2$. While the frequency dependence in the region below this discontinuity was usually different from the f^{-4} predicted, the higher frequency dependence was clearly distributed around the expected value of f^{-6}. Indeed, a weighted average of all measurements led to a final value of -5.6 ± 0.01.

IV. AMBIENT NOISE CHARACTERISTICS

A. Spectral behavior with wind speed

Because the geophysical data required to effectively evaluate the properties of the transfer function in Eq. (4) are not available, we can, as a first approximation, assume with Urick[23] that the sea bottom is an infinite surface, radiating and responding to plane waves incident from above or below, and use the observed microseism levels to establish the associated pressure field in a comparison of the results with other ambient noise measurements.

The results for the event of 16–20 October (see Fig. 2) are shown in Fig. 7. Included for comparison is a spectrum taken on 24 October during the period of high activity later in the month. In this and in subsequent figures, spectrum levels are related to a 1-Hz bandwidth and derived from the equivalent form of Eq. (4), with f expressed in hertz.

Figure 7 demonstrates very well the nature of the spectral development in an event of this kind. At 0340Z on 17

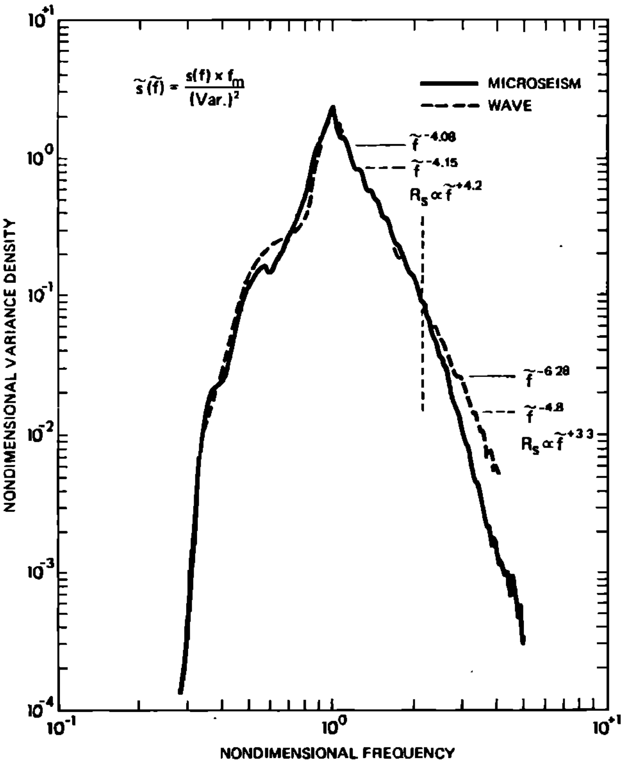

FIG. 6. Nondimensionalized spectral functions for the S group of spectra.

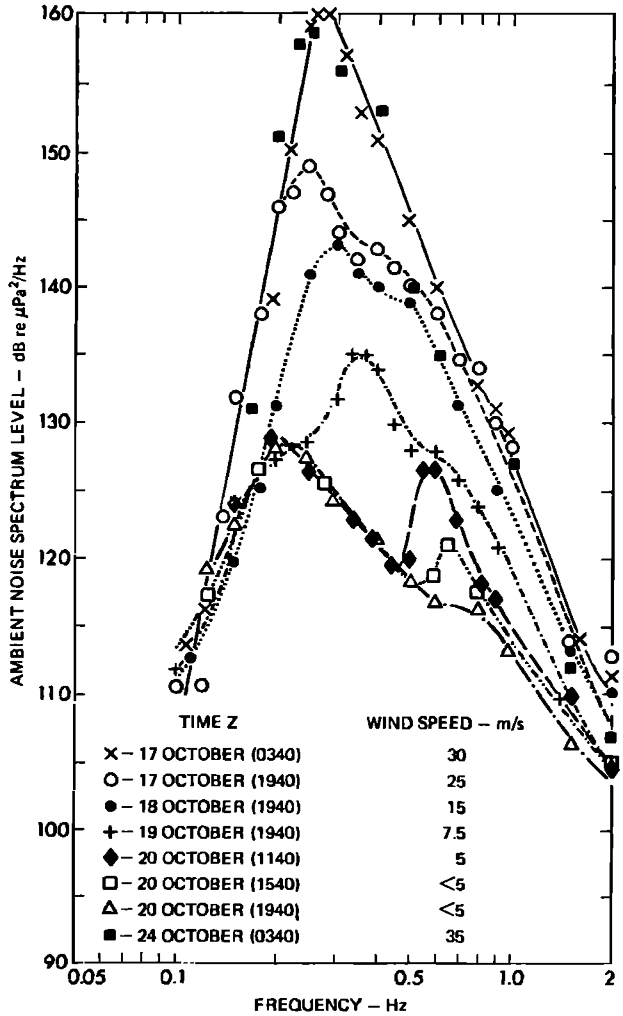

FIG. 7. Ambient noise levels derived from seismic spectra as a function of wind speed.

October, the wave and seismic levels are high. As the wind drops, the spectral peak initially decreases in magnitude without shifting significantly in frequency, but evidence of movement in the peak is apparent by 1940Z on 18 October. Thereafter, the peak continues to decrease and shift to higher frequencies.

By 1940Z on 19 October, the seismic activity associated with the ever present low-frequency wave energy becomes visible. This component of the wave field has its origin primarily in distant southwesterly swells from the Southern Ocean,[27,28] but energy will also be present from distant fetches throughout the Tasman Sea.

As the local sea continues to decay, this residual low-frequency energy becomes more and more dominant. In the Maui region, wave and seismic activity rarely drops below the level represented by the spectrum of 1940Z on 20 October (significant wave height approximately 1.2 m). The statistics of five years of data show indeed that the average significant wave height is 2–3 m.[27] This background will therefore generally obscure wind-dependent effects at low wind speeds. Background levels are much lower on the east coast of New Zealand,[30] but high residual swell levels can be expected in most open ocean areas.

While the double frequency relationship establishes the source of the low-frequency component of the residual noise field as the background swell experienced in the area, evidence such as a much lower spectral peak power ratio indicates that the mechanism leading to the generation of the seismic pressure field is clearly different. This lower ratio and the absence of an angular distribution of energy in the case of swell lead to the conclusion that coastal reflection sets up the opposing wave field in this case. The high dependence of coastal reflection of ocean waves on coastal geometry and the degree of exposure to distant fetches will influence the level of this background noise component in coastal regions. These questions are examined in detail elsewhere.[30]

B. Comparison with other data

The ambient noise levels of Fig. 7 are compared with other ambient noise data in Fig. 8. The data selected for comparison are those considered to be most relevant on the basis of the review carried out by Nichols.[17] Recent data from Talpey and Worley (not plotted) follow these trends closely.[37]

Within the 0.1- to 2-Hz bandwidth, the Talpey and Worley and the Eleuthera data fall convincingly within the range of the New Zealand spectra. Further, the wind depen-

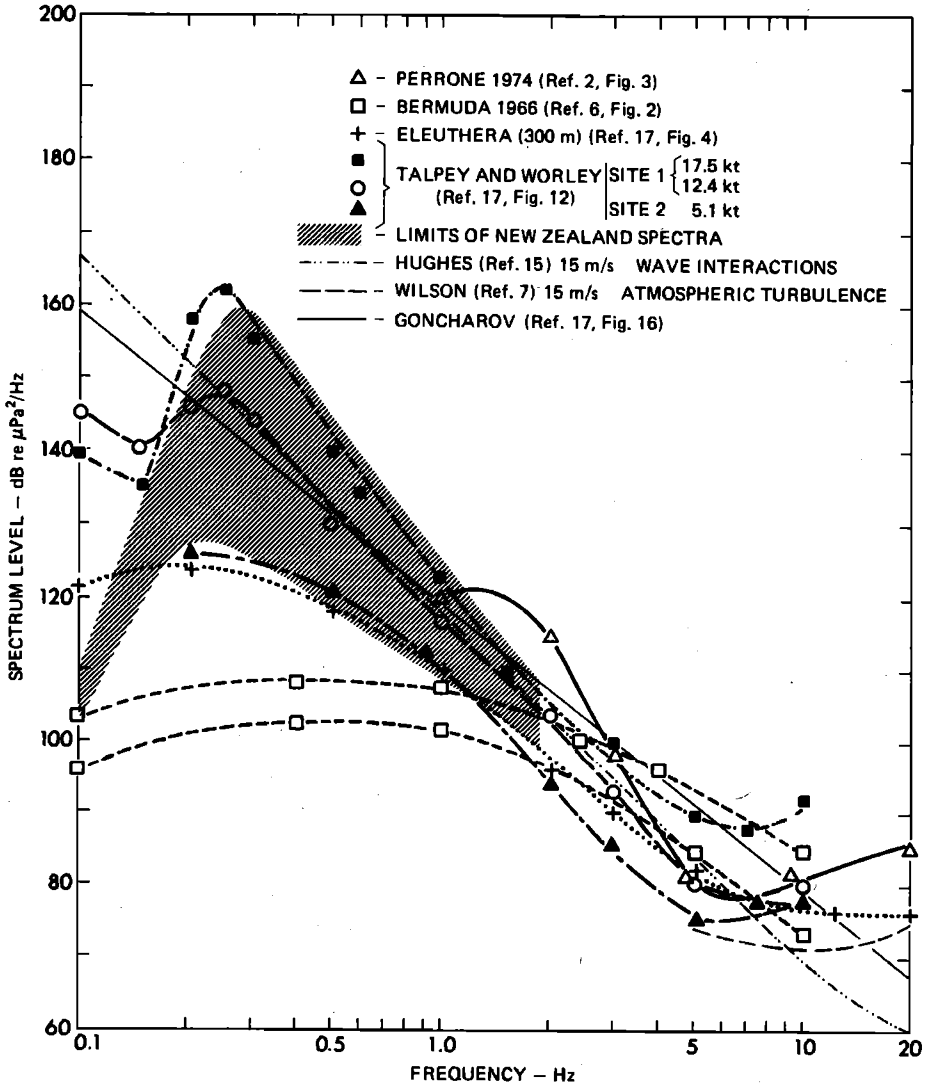

FIG. 8. Comparison of various ambient noise data sets.

dence is of the same form. However, the rise in spectral level below 0.1 Hz is not observed in the seismic results for which a low-frequency plotting limit of 0.09 Hz is imposed. Above 2 Hz, the seismic data are effected by unrelated effects and are not included, but it is clear that the trends above 2 Hz are comparable in all cases.

The Perrone and Bermuda data do not conform so well, but the authors acknowledge uncertainties in the recording system below 1.0 Hz.

Results from the east coast of New Zealand, where residual wave and seismic levels are lower and hydrophone information is also available, are being processed and will be reported in due course.

V. COMPARISON WITH THEORETICAL PREDICTIONS

A. Noise level

The two currently favored theories relating wind and surface waves to ambient noise generation at low frequencies are represented by the papers of Isakovich and Kuryanov[4] and Wilson,[7] on the one hand, and Brekhovskikh,[12] Hughes,[14] and Lloyd,[15] on the other.

The mechanism proposed by Isakovich and Kuryanov involves the generation of noise by turbulent pressure fluctuations in the atmosphere near the ocean surface. Wilson[7] modified the original theory and used more modern wave-height spectral information in computing the noise field. The calculations have been the subject of debate,[38,39] but, for the present purposes, his predicted levels of noise induced by atmospheric turbulence for a wind speed of 15 m/s (30 kn) are shown in Fig. 8 and to higher frequencies are shown in Fig. 9. In the 20-down to 10-Hz range, predictions agree reasonably with observations, but, below 10 Hz, fall below measured values. Wilson concludes that atmospheric turbulence is the dominant source of wind generated noise above 5 Hz and suggests, with others, that surface wave–wave interactions are responsible between 1 and 5 Hz.

Also shown in Figs. 8 and 9 is a noise prediction presented by Nichols[17] (his Fig. 16), based on Goncharov's[16] theory of the interaction of surface waves and ocean turbulence. This is not markedly different from that based on the nonlinear interaction of surface waves alone, but a distinction between the two mechanisms can be drawn on the basis of the frequency characteristics of the noise spectrum (see Sec. V B).

Early theoretical estimates of ocean noise generated by nonlinear interactions do not agree closely with measured values, either. However, recently, Hughes,[14] incorporating modern surface wave data and allowing for surface–bottom reflections, has produced revised estimates. His predicted spectrum for a 15-m/s wind (extrapolated below 1 Hz) is also shown in Figs. 8 and 9. Below 5 Hz, his predicted values agree closely with the Talpey and Worley spectrum (average wind speed of 12.4 kn) and the Maui spectrum of 18 October (1940Z) for which the wind speed was 15 m/s (30 kn) (see Figs. 7 and 8). Above 10 Hz, the theoretical values fall below the experimental data. It is to be noted, however, that Lloyd has shown Hughes' prediction to be too high by a factor of 2. Hughes' original prediction and Lloyd's amendment are shown in Fig. 9.

At first, the close agreement between the present experimental levels and the theoretical predictions at frequencies below 10 Hz might be seen as fortuitous. The bottom amplification factor included in the theoretical predictions shown in Figs. 8 and 9 [see Ref. 14, Eq. (42)] depends upon various parameters, including water depth, and there is uncertainty in assigning values to these parameters appropriate to the Maui area. A bottom reflection coefficient of unity is also assumed, which will not be appropriate to the situation involved.

It is, however, instructive to compare the acoustic pressure levels derived from the ground displacement with those calculated using the observed values of $Sa(f_W)$ and based on Eq. (1). For spectra with a close 2:1 frequency relationship, we find that, at frequencies close to the spectral peak, the two

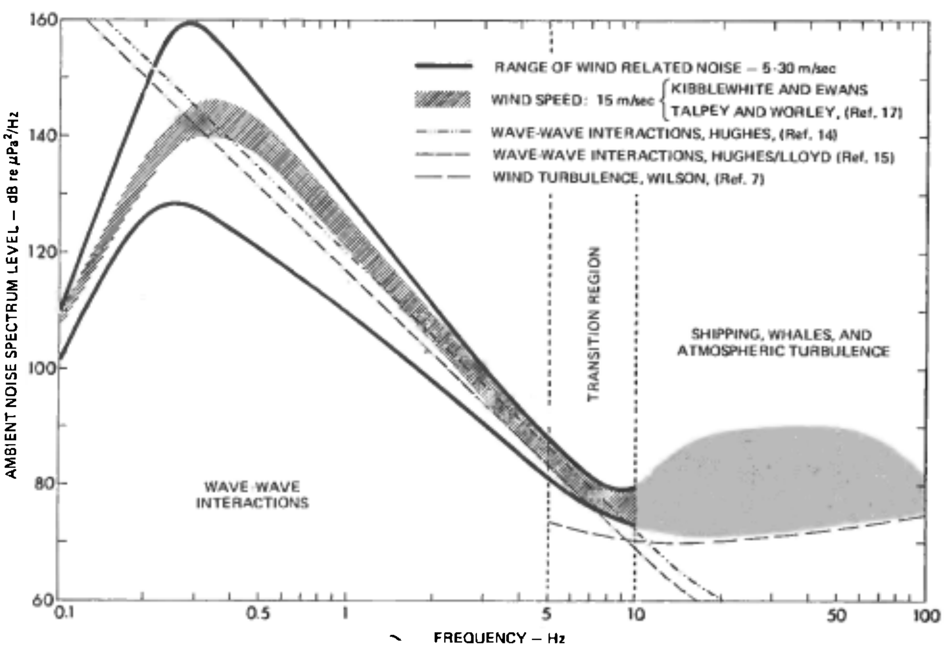

FIG. 9. Suggested form of the ambient noise spectrum below 100 Hz in mid-ocean waters.

values agree to within a few decibels. At higher frequencies ($0.4 < f < 1.0$ Hz), the pressure levels derived from the wave field are typically 10–15 dB below those deduced from the seismic spectrum.

If we assume a 10- to 15-dB bottom amplification factor to bring the high-frequency levels into agreement, the values near the peak become too high by about the same amount (8–12 dB). Two possible explanations can be considered. The first is that it is not sufficient to consider only the effect of the bottom amplification on the incident pressure field generated by the ocean-wave interactions. With a reflection coefficient less than unity, the frequency dependence of the bottom transfer function must be considered. In Eq. (4), a simple linear frequency dependence was assumed, but it is conceivable that an additional frequency dependence is embodied in K_2. A more complex frequency dependence in the transfer function of a form which would remove the small anomaly observed between the pressure fields evaluated from Eqs. (1) and (4) is not unexpected, although its precise nature is unknown. Alternatively, it is conceivable that the two equilibrium ranges in the wave spectrum mentioned earlier (see Fig. 6) account for the mismatch between the two frequency regions in the noise spectrum. This would imply that the wave spectral interactions differ in some way in each frequency range, leading to a different power dependence in the frequency parameter in Eq. (4). Certainly nonlinear wave–wave interactions are known to involve primarily frequency components near the spectral peak.[24] It is even possible that a combination of such effects is involved. On the evidence available, it is not possible to resolve the question. It can be noted, however, that recently Burgess and Kewley[40] have shown that ambient noise levels are sensitive to bottom reflectivity, and that an overall frequency dependence of the form required to remove the anomaly between the pressure fields as calculated from Eqs. (1) and (4) is compatible with what is known of the sedimentary structure in the area. The inflexion around 0.5 Hz apparent in Fig. 7 is suggestive of a transfer function with a narrow peak, as would be required.

With the unknowns involved, the quantitative agreement obtained is considered reasonable. It is obvious, however, that the Hughes–Lloyd prediction in Fig. 9 tends to fall below the experimental data [and the predictions based on Eq. (1)], around the spectral peak. It is believed that this arises because of the nature of the wave field in the Maui region. The present study has shown, *inter alia*, that a peak enhancement factor as first discussed by Hasselmann *et al.*[35] is also necessary for an accurate analytical description of the seas on the west coast of New Zealand.[29,30] The effect of the peak enhancement factor decreases rapidly away from the peak but its value of approximately 2 for the Maui seas means that, at the spectral peak, the pressure field based on Eq. (1) will be greater by a factor of around 6 dB than the Hughes prediction shown in Fig. 9.

In spite of the difficulty with absolute levels, we have additional support for the role of wave–wave interactions below 5 Hz, in the theoretical dependence of the observed noise levels on sea state. According to Eq. (1), the acoustic pressure level should be proportional to the second power of the surface-wave spectral density $\{$i.e., to $[Sa(\sigma)]^2\}$. As discussed earlier, this relationship is confirmed by the results of this study (see Fig. 5). Additional evidence is provided by the spectral frequency dependence to be discussed below.

We note finally that the bottom amplification referred to above will have implications for Wilson's[41] theoretical curve presented in Figs. 8 and 9. This prediction assumes a seabed of poor reflecting properties and, hence, no bottom enhancement.[41] With allowance for bottom amplification, Wilson's theoretical curve will be in closer agreement with observed values.

B. Frequency dependence

Equations (1) and (4) imply that, above the peak, the frequency dependence of the acoustic noise field (seismic or pressure) depends on the high-frequency slope of the ocean-wave spectrum. The ratio R_s should, however, display a fourth or third power dependence on frequency for the ground displacement and acoustic pressure spectra, respectively. This question was considered earlier in an examination of the ratio R_s using nondimensionalized spectra. This analysis showed that, in the region above the spectral peak, the frequency dependence of R_s supports the nonlinear wave interaction hypothesis.

Further, the detailed analysis of the nondimensional ocean-wave spectra in the Maui region[30] established two intervals in the equilibrium range (with slopes of approximately -4 and -5)—see Fig. 6. Using a mean value of -4.5 for the high-frequency slope of the ocean-wave field $Sa(\sigma)$, one would expect $Sp(\omega)$ in Eq. (1) to display a frequency dependence of approximately ω^{-6}, corresponding to a spectral slope of around 18 dB/oct. Figure 7 shows that, at high wind speeds, the spectral slope is of this order between 0.3 and 1 Hz.

Finally, Goncharov's theory of ocean turbulence predicts a spectral slope of ω^{-4}. The evidence from spectral slope information therefore provides further support for Brekhovskikh's proposal that wave–wave interactions are the noise generating mechanism at frequencies below 5 Hz.

C. Region above 5 Hz

Between 5–10 Hz, another mechanism is obviously beginning to influence the noise level. As Wilson has pointed out, the characteristics of atmospheric turbulence appear to account for the trends observed in this region.

In the absence of any other source, the characteristics of the two noise mechanisms lead one to expect a minimum in the noise spectrum between 5 and 10 Hz. Such a minimum is apparent in Fig. 8. It is, furthermore, a definite feature of New Zealand hydrophone data currently being processed and is also strikingly demonstrated in some recent Canadian results (I. Frazer,[42] personal communication).

The nature of the spectrum above 5 Hz will, however, depend on the relative levels of the two wind-related noise components, and any shipping and biological activity in the region. The effect these combined sources might be expected to produce on a mid-depth midocean noise spectrum at frequencies below 100 Hz is shown in Fig. 9. At these frequencies, the distortion introduced by volume attenuation will be minor.

Finally, it is an observational fact that the rise in energy at very low frequencies becomes apparent only below 4–5 Hz, irrespective of wind speed, but increases rapidly below this frequency. This is another reason for concluding that Wilson's theoretical predictions, without a correction for bottom enhancement, are at least 10–15 dB too low for most regions.

VI. SUMMARY

It has been proposed that nonlinear wave–wave interactions and/or atmospheric turbulent pressure fluctuations provide the most promising explanations for the ocean noise generated in the region below 10 Hz. However, the experimental data covering this part of the spectrum are limited, and, although the evidence is supportive, it has not been possible to provide positive confirmation to date. The main problems arise through the experimental difficulties involved with conventional hydrophone installations, the fact that most noise measurements have been of only short duration, and in limitations in the supporting environmental data.

An ocean environment possessing particular properties and long-term recordings so critical to the resolution of complex geophysical phenomena were features of the present experiment, and they have provided clarification of the roles of the two wind-related noise generating mechanisms operating at very low frequencies.

Specifically, it has been demonstrated that surface wave–wave interactions are the dominant mechanism of noise generation from 0.1–5 Hz. The mechanism is also responsible for the generation of ocean-induced microseisms.

It has been shown further why, as has been often observed,[43] the low-frequency noise field correlates better with the wind than with sea state and why there is effectively no phase lag. The nonlinear wave interactions, which adjust the sea state, occur immediately after a change in the wind field, but the ocean-wave spectrum takes some time to accommodate to these processes.

The noise field is, however, not a simple function of wind speed. A shift in bearing in a moderate wind field has been shown to have an effect on the sea noise comparable with that produced by a large change in wind speed on a constant bearing. Indeed, several distinct interplays between wind speed and noise level can now be identified.

The greatest wind related noise levels occur when a 180° shift in a wind of long duration brings a growing sea into direct opposition with the one already established. (This effect has been reported before,[44] but its real significance has only been demonstrated with the long-term data of the present experiment.) While the two wave fields interact, the noise levels remain very high, but drop quickly to levels some 20 dB lower as the new wave field becomes dominant. This new level of activity reflects the nonlinear processes active within the single wave field and the noise is now related more simply to wind speed.

The processes generating the underwater sound field, where two opposing seas are interactive, decay as the new wave field becomes dominant. As these processes decay, noise levels reach a lower level set by the same processes active within the single wave field. This noise field is wind dependent but, even at low wind speeds, a residual noise field is observed—see Fig. 7. This background level will vary from region to region and, in fact, differs by an order of magnitude from the exposed west coast of New Zealand to the quieter seas on the east coast.

Between 5–10 Hz, another wind-dependent process influences the noise field. The present evidence supports earlier claims that, in this frequency region, the effects of atmospheric turbulence begin to be manifest. The induced noise field is now related on a 1:1 frequency basis with the fluctuations in the exciting turbulence field and displays different frequency and wind-dependent characteristics.

The combined effects of nonlinear interactions and atmospheric turbulence produce a minimum in the noise spectrum around 10 Hz. The visibility of the effects of atmospheric turbulence depends, however, on the influence of shipping and other sources on the noise field.

A close equivalence between seismic levels and the wave-induced acoustic levels at the seabed at frequencies below 10 Hz has implications for the modeling of the ocean noise field. In the present experiment, the levels of ground motion recorded by a land-based sensor correlated closely with the exciting pressure field. Furthermore, on occasions, components in the seismic spectrum could be correlated with wave activity on the east coast of New Zealand,[27,30] confirming many earlier reports that, even in complex geological structures, wave induced seismic signals suffer little attenuation in transmission to long distances. The possibility exists, therefore, for energetic storms to influence the noise field at distant regions in the ocean. This possibility is especially marked if the wave interaction occurs on the continental shelf. Downslope propagation, as proposed by Wagstaff,[45] could, in this case, occur for any energy reradiated into the water column. The possibility also exists for the equivalent of *T*-phase transmission transferring energy into the sound channel.

In conclusion, it is of interest to observe that, once again, the study of a problem in ocean acoustics has been not only dependent on input from, but also provided a contribution to, oceanography. In this case, the properties of the ambient noise field have provided information on mesocale processes in the ocean-wave field.

ACKNOWLEDGMENTS

This investigation was carried out as part of the Maui Development Environmental Study conducted by The University of Auckland for Shell BP and Todd Oil Services, Ltd. acting on behalf of Maui Development, Ltd. Other agencies contributed to the program. In particular, the NZ Meteorological Service provided the weather and wind reports and the University Grants Committee assisted in purchasing some of the specialized instrumentation. The contributions of many individuals are gratefully acknowledged. Special thanks are extended to the staff of the Oaonui Production Station for routine supervision of the recording instrumentation, P. G. Dolden for maintenance of the wave recorder, and Dr. M. D. Johns, D. A. Ash, and D. B. Coup for computational assistance in analysis. The project could never have been completed successfully, however, without the technical skills and enthusiasm of D. A. Jones, who not only designed and maintained the shore recording instrumentation, but also provided general management support to this and other programs throughout the whole period of the environmental study.

[1]G. M. Wenz, "Acoustic Ambient Noise in the Ocean: Spectra and Sources," J. Acoust. Soc. Am. 34, 1936–1955 (1962).
[2]A. J. Perrone, "Infrasonic and Low-Frequency Ambient Noise Measurements on the Grand Banks," J. Acoust. Soc. Am. 55, 754–758 (1974).
[3]K. Hasselmann, "A Statistical Analysis of the Generation of Microseisms," Rev. Geophys. 1, 177–210 (1963).
[4]M. A. Isakovich and B. F. Kur'yanov, "Theory of Low Frequency Noise in the Ocean," Sov. Phys. Acoust. 16, 49–58 (1970).
[5]W. Strawderman, "Turbulent Air Flow Induced Sea Noise," NUSC Technical Document 12-190-74, Naval Underwater Systems Center, New London, CT, 28 June 1974.
[6]N. Yen and A. J. Perrone, "Mechanisms and Modelling of Wind-Induced Low Frequency Ambient Sea Noise," NUSC Tech. Rep. 5833, Naval Underwater Systems Center, New London, CT (13 February 1979).
[7]J. H. Wilson, "Very Low-Frequency (VLF) Wind-Generated Noise Produced by Turbulent Pressure Fluctuations in the Atmosphere Near the Ocean Surface," J. Acoust. Soc. Am. 66, 1499–1507 (1979).
[8]M. Miche, "Mouvements Ondulatoires de la Mer en Profondeur Constante ou Decroissante," Ann. Ponts Chaussees 114, 25–87 (1944).
[9]M. S. Longuet-Higgins, "A Theory of the Origin of Microseisms," Philos. Trans. R. Soc. London Ser. A 243, 1–35 (1950).
[10]J. N. Nanda, "The Origin of Microseisms," J. Geophys. Res. 65, 1815–1820 (1960).
[11]J. Darbyshire and E. O. Okeke, "A Study of Primary and Secondary Microseisms Recorded in Anglesey," Geophys. J. R. Astron. Soc. 17, 63–92 (1969).
[12]L. M. Brekhovskikh, "Underwater Sound Waves Generated by Surface Waves in the Ocean," Izv. Atmos. Ocean. Phys. 2, 582–587 (1966) (translated by J. Gollob).
[13]E. Y. Harper and P. G. Simpkins, "On the Generation of Sound in the Ocean by Surface Waves," J. Sound Vib. 37, 185–193 (1974).
[14]B. Hughes, "Estimates of Underwater Sound (and Infrasound) Produced by Nonlinearly Interacting Ocean Waves," J. Acoust. Soc. Am. 60, 1032–1039 (1976).
[15]S. P. Lloyd, "Underwater Sound from Surface Waves According to the Lighthill–Ribner Theory," J. Acoust. Soc. Am. 69, 425–435 (1981).
[16]V. V. Goncharov, "Sound Generation in the Ocean by the Interaction of Surface Waves and Turbulence," Izv. Atmos. Ocean. Phys. 6, 1189–1196 (1970) (translated by F. Goodspeed).
[17]R. H. Nichols, "Infrasonic Ambient Ocean Noise Measurements: Eleuthera," J. Acoust. Soc. Am. 69, 974–981 (1981).
[18]F. I. Monakhov and V. M. Zhak, "The Mechanism of Microseism Generation from the Sea-Floor Observations off the Island of Shikotan," Izv. Earth Phys. 13(4), 290–292 (1977).
[19]F. I. Monakhov, V. M. Zhak, and V. A. Nesterov, "Mechanism of Generation of Microseism by a Storm during the Period October 10–11, 1976, near Island Shikotan," Izv. Earth Phys. 14(4), 302–303 (1978).
[20]A. A. Ostrovsky, "On Some Characteristics of Microseism Sources," Izv. Earth Phys. 15(11), 825–828 (1979).
[21]G. V. Latham and A. I. Mowroozi, "Waves, Weather and Ocean-Bottom Microseisms," J. Geophys. Res. 73, 3945–3957 (1968).
[22]G. H. Sutton, W. G. McDonald, D. D. Prentiss, and S. N. Thanos, "Ocean-Bottom Seismic Observations," Proc. IEEE 53, 1909–1921 (1965).
[23]R. J. Urick, "Seabed Motion as a Source of Ambient Noise Background in the Sea," J. Acoust. Soc. Am. 56, 1010–1011 (1974).
[24]K. Hasselmann, D. B. Ross, P. Muller, and W. Sell, "A Parametric Wave Prediction Model," J. Phys. Ocean. 6, 200–228 (1976).
[25]D. O. Zopf, H. C. Creech, and W. H. Quinn, "The Wavemeter: A Land-Based System for Measuring Nearshore Ocean Waves," Mar. Tech. Soc. J. 10(4), 19–25 (1976).
[26]A. C. Kibblewhite and R. N. Denham, "Experiment on Sound Propagation in Shallow Water Under Isovelocity Conditions," J. Acoust. Soc. Am. 40, 1337–1344 (1966).
[27]A. C. Kibblewhite, P. R. Bergquist, B. A. Foster, M. R. Gregory, and M. C. Miller, "Maui Development Environmental Study: Report on Phase 2, 1977–1981," University of Auckland, New Zealand (October 1982).
[28]S. M. Chiswell and A. C. Kibblewhite, "Ocean Wave Studies in Western Cook Strait," NZ J. Mar. Freshwater Res. 14(4), 417–425 (1980).
[29]S. M. Chiswell and A. C. Kibblewhite, "Spectra of the Fully Developed Wind Generated Ocean Wave Field West of Central New Zealand," N. Z. J. Mar. Freshwater Res. 15(1), 81–84 (1981).
[30]K. C. Ewans, "Ocean Waves, Microseisms, and Their Interrelations," Doctoral dissertation, University of Auckland, New Zealand (1984).
[31]M. S. Longuet-Higgins, "On the Statistical Distribution of Heights of Sea Waves," J. Mar. Res. 11(3), 245–266 (1952).
[32]G. L. Tyler, C. C. Teague, R. H. Stewart, A. M. Peterson, W. H. Munk, and J. W. Joy, "Wave Directional Spectra from Synthetic Aperture Observations of Radio Scatter," Deep Sea Res. 21, 989–1016 (1974).
[33]G. M. Hidy and E. J. Plate, "Frequency Spectrum of Wind-Generated Waves," Phys. Fluids 8, 1387–1389 (1965).
[34]P. C. Liu, "Normalized and Equilibrium Spectra of Wind Waves in Lake Michigan," J. Phys. Ocean. 1(4), 249–257 (1971).
[35]K. Hasselmann, J. P. Barnett, E. Bouws, H. Carlson, D. E. Cartwright, K. Enke, J. A. Ewing, H. Glenapp, D. E. Hasselmann, P. Kruseman, A. Meerburg, P. Muller, D. J. Olbers, K. Richter, W. Sell, and H. Walden, "Measurements of Wind-Wave Growth and Swell Decay during the Joint North Sea Wave Project (JONSWAP)," Dent. Hydrogr. Z. Suppl. A 8, No. 12 (1973).
[36]G. Z. Forristall, "Measurements of a Saturated Range in Ocean Wave Spectra," J. Geophys. Res. 86, 8075–8084 (1981).
[37]T. E. Talpey and R. D. Worley, "Infrasonic Ambient Noise Measurements in Deep Atlantic Water," J. Acoust. Soc. Am. 75, 621–622 (1984).
[38]D. H. Cato, "Comments on 'Very Low-Frequency (VLF) Wind-Generated Noise Produced by Turbulent Pressure Fluctuations in the Atmosphere Near the Ocean Surface,'" J. Acoust. Soc. Am. 77, 1783 (1981).
[39]J. H. Wilson, "Rebuttal to 'Comments on Very Low-Frequency (VLF) Wind-Generated Noise Produced by Turbulent Pressure Fluctuations in the Atmosphere Near the Ocean Surface,'" J. Acoust. Soc. Am. 70, 1785 (1981).
[40]A. S. Burgess and D. J. Kewley, "Wind-Generated Surface Noise Source Levels in Deep Water East of Australia," J. Acoust. Soc. Am. 73, 201–210 (1983).
[41]J. H. Wilson, "Wind-Generated Noise Modeling," J. Acoust. Soc. Am. 73, 211–216 (1983).
[42]I. Frazer (personal communication) (1983).
[43]J. A. Shooter and M. L. Gentry, "Wind-Generated Noise in the Parece Vela Basin," J. Acoust. Soc. Am. 70, 1757–1761 (1981).
[44]V. N. Tabulevich, "Swell, Opposing Winds and Microseisms," Izv. Geophys. Ser. No. 11, 1667–1675 (1963).
[45]R. A. Wagstaff, "Low-Frequency Ambient Noise in the Deep Sound Channel—The Missing Component," J. Acoust. Soc. Am. 69, 1009–1013 (1981).